Articles

Origin of the Chlorophyll *b* Formyl Oxygen in *Chlorella vulgaris*†

Mark A. Schneegurt‡ and Samuel I. Beale*,§

DowElanco, Greenfield, Indiana 46140, and Division of Biology and Medicine, Brown University, Providence, Rhode Island 02912

Received July 15, 1992; Revised Manuscript Received September 4, 1992

ABSTRACT: Chlorophyll (Chl) *b* is an accessory light-harvesting pigment of plants and chlorophyte algae. Chl *b* differs from Chl *a* in that the 3-methyl group on ring B of Chl *a* is replaced by a 3-formyl group on Chl *b*. The present study determined the biosynthetic origin of the Chl *b* formyl oxygen in in vivo labeling experiments. A mutant strain of the unicellular chlorophyte *Chlorella vulgaris*, which can not synthesize Chls when cultured in the dark but rapidly greens when transferred to the light, was grown in the dark for several generations to deplete Chls, and then the cells were transferred to the light and allowed to form Chls in a controlled atmosphere containing $^{18}O_2$. Chl *a* and Chl *b* were purified from the cells and analyzed by high-resolution mass spectroscopy. Analysis of the mass spectra indicated that over 76% of the Chl *a* molecules had incorporated an atom of ^{18}O. For Chl *b*, 58% of the molecules had incorporated an atom of ^{18}O at one position and 34% of the molecules had incorporated an atom of ^{18}O at a second position. These results demonstrate that the isocyclic ring keto oxygen of both Chl *a* and Chl *b*, as well as the formyl oxygen of Chl *b*, is derived from O_2.

Chl[1] *b* is a ubiquitous accessory light-harvesting pigment in plants and chlorophyte algae. Chl *b* differs from Chl *a* in that the 3-methyl group on ring B of Chl *a* is replaced by a 3-formyl group on Chl *b* (Figure 1). Various researchers have suggested that the Chl *b* precursor on which the methyl-to-formyl conversion occurs is Chl *a* (Godnev et al., 1960; Akoyunoglou et al., 1967; Shlyk, 1971; Shlyk et al., 1975), Chlide *a* (Oelze-Karow et al., 1978; Oelze-Karow & Mohr, 1978; Duggan & Rebeiz, 1982), Chl *a* containing a geranylgeranyl group that has not yet been reduced to phytyl (Benz et al., 1984), or Pchlide *a* (Bednarik & Hoober, 1985, 1986). It is not clear whether the conversion occurs before or after esterification of the 7-propionate group with phytol or a phytol precursor (Beale & Weinstein, 1990).

The 3-formyl group of Chl *b* is presumably formed from the 3-methyl group of a precursor by oxidation, and the oxygen atom may be derived from either O_2 or H_2O. Because Chl *b* occurs only in aerobic organisms, it has been suggested that O_2 is involved in its formation (Castelfranco & Beale, 1983). One report found that Chl *b* formation occurred at a slower rate in an oxygen-depleted atmosphere (Aronoff & Kwok, 1977). Further support for the role of O_2 is supplied by more recent studies in which O_2 was required for in vitro conversion of Pchlide *a* to Chlide *b* in extracts of *Chlamydomonas reinhardtii* (Bednarik & Hoober, 1985; 1986).

We have investigated the origin of the Chl *b* formyl oxygen atom by analyzing the mass spectra of Chls synthesized by the unicellular chlorophyte, *Chlorella vulgaris*, in an $^{18}O_2$-enriched atmosphere. The results indicate that the isocyclic ring keto oxygen of both Chl *a* and Chl *b* is derived from O_2 and that the Chl *b* formyl oxygen is also derived from O_2.

EXPERIMENTAL PROCEDURES

Cell Culture and Preparation. Chlorella vulgaris Beijerinck strain C-10 was maintained in the dark as previously described (Weinstein & Beale, 1985). Strain C-10 forms normal amounts of Chls in the light but is completely unable to form Chls when cultured in the dark (Bryan & Bogorad, 1963). The growth rate in dextrose-containing culture medium is the same (10-h doubling time) in the light or dark. For ^{18}O-labeling experiments, the cells from 500 mL of dark-grown culture were collected in the exponential growth phase by centrifugation, washed with growth medium from which dextrose was omitted, and resuspended to a volume of 330 mL in growth medium lacking dextrose and supplemented with 10 μM DCMU.

Description of the Reaction Vessel. $^{18}O_2$-Labeling experiments were performed in a 500-ml round-bottom four-neck flask. One of the necks was fitted with a stopcock which, when connected to a separate three-way valve, allowed the reaction vessel to be alternately evacuated with a vacuum pump and filled with O_2-free N_2. $^{18}O_2$ was introduced to the vessel through a tee-shaped fitting. A sealed flask containing 100 mL of $^{18}O_2$ (at atmospheric pressure) was connected to one of the horizontal arms, and the other horizontal arm was fitted with a sealed flexible tube harboring a thin aluminum rod. At the appropriate time, the rod was used to break the glass seal of the $^{18}O_2$ flask without opening the apparatus to the external atmosphere. The third neck of the vessel was fitted with a thermometer. For some experiments, the fourth neck was fitted with a Clark-type oxygen sensor; in others, it was stoppered. The reaction apparatus had a total volume of 730 mL (including the 100-mL $^{18}O_2$ flask). Thus, with 330 mL of liquid culture, the gas phase of the system (400 mL)

† This work was supported in part by Grant DCB92-03253 from the National Science Foundation.

* To whom correspondence should be addressed.

‡ DowElanco. Current address: Department of Biological Sciences, Purdue University, West Lafayette, IN 47907.

§ Brown University.

[1] Abbreviations: Chl, chlorophyll; Chlide, chlorophyllide; DCMU, 3,4-dichlorophenyl-1,1-dimethylurea; NPG, natriated poly(ethylene glycol); Pchlide, protochlorophyllide.

0006-2960/92/0431-11677$03.00/0 © 1992 American Chemical Society

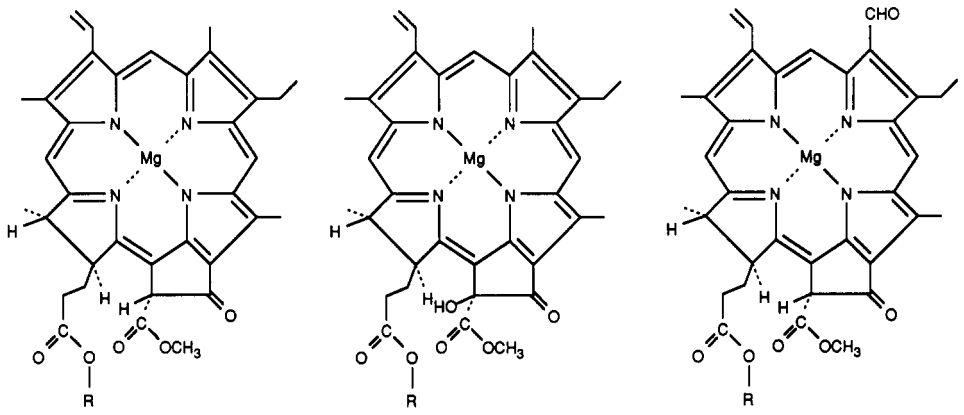

FIGURE 1: Structures of the compounds referred to in the text. R = phytyl ($C_{20}H_{39}$-).

could be brought to nearly atmospheric pressure of O_2 and N_2 when the contents of the 100-mL $^{18}O_2$ flask were added to the evacuated apparatus and then the pressure was raised to atmospheric level with N_2.

The reaction vessel was illuminated by an incandescent lamp at 30 μmol of photons m^{-2} s^{-1}, and reflective foil was placed on the side opposite the light source. A tank containing 1% (w/v) aqueous $CuSO_4$ was placed between the light source and the reaction vessel to filter out heat-producing radiation. The culture was agitated by stirring with a magnetic stir bar. The stirring motor was thermally isolated from the reaction vessel.

^{18}O-Labeling Incubation Conditions. Washed cells, suspended in growth medium lacking glucose and containing 10 μM DCMU, were introduced into the reaction vessel and allowed to incubate with stirring and at full illumination for 30 min before the vessel was sealed. The vessel was then alternately evacuated and flushed with N_2 four times and finally evacuated and disconnected from the vacuum pump. The seal on the $^{18}O_2$ flask was broken with the aluminum rod and N_2 was then carefully introduced into the flask until atmospheric pressure was reached. The cells were maintained under continuous illumination in this environment overnight.

Chl Extraction and Purification. After incubation, the reaction vessel was thoroughly cooled on ice before it was opened. The cells were harvested by centrifugation, and pigments were rapidly extracted with three 25-mL portions of ice-cold methanol by vortex suspension and centrifugation. The extracted pigments were immediately partitioned into hexane (25 mL) with the addition of water (25 mL). The hexane fraction was washed 3 times with water to remove traces of methanol, and the solvent was evaporated to incipient dryness under a stream of dry N_2. The residue was stored under N_2 in the dark at −20 °C. For HPLC separation, the pigments were dissolved in ice-cold methanol and applied to a C_{18} reverse-phase column (25 cm long × 4.6 mm diameter; 5-μm particle size; Supelco, Inc., Bellefonte, PA) using a Waters instrument (Models 600E and 700; Millipore Corp., Bedford, MA). Chls were eluted with an isocratic flow of methanol:water (98:2 v/v) at 1 mL/min. Elution was monitored at 660 nm using a Waters 991 photodiode array detector, and peak fractions were collected manually. The appropriate fractions were brought to incipient dryness with a stream of dry N_2 (with the addition of acetone to facilitate water loss). Samples were stored under N_2 in the dark at −20 °C. Throughout the purification, all procedures were carried out under dim light, the time of exposure of the Chls to methanol was minimized, and the temperature was kept as low as possible to minimize the formation of Chl allomers (Holt, 1958; Schaber et al., 1984).

Mass Spectral Analysis. FAB mass spectra were generated with a VG ZAB-2SE mass spectrometer (Fisons Instruments, Inc., Danvers, MA) and acquired by a VG OPUS 2000 data system. Samples were dissolved in 3-nitrobenzyl alcohol and delivered to the ion source via a direct insertion probe as previously described (Hunt & Michalski, 1990). NPG was used as the internal standard. A Cs ion gun was used to deliver energetic particles (12 keV net) for bombardment of the sample. The mass spectrometer was operated at an accelerating voltage of 8 kV, with positive ion detection at the point of double focus of the two sectors. Source and collector slits were adjusted to yield a resolution (10% valley) of 1 part in 10 000.

Other Methods. Spectrophotometric measurements were performed on a Cary 2290 instrument (Varian Associates, Inc., Sunnyvale, CA), and the Chl absorption spectra were recorded in methanol. The spectral data were further analyzed by Bessel deconvolution using the Spectra Calc data package (Galactic Industries Corp., Salem, NH).

Materials. $^{18}O_2$ was purchased from Du Pont–NEN (Boston, MA) and was certified to be 97–98% isotopically pure. All solvents were HPLC grade. Other chemicals were of reagent grade.

RESULTS

Reaction Conditions. The *Chlorella* C-10 mutant cells used in this study had been grown in the dark for several generations and contained insignificant amounts of Chls at the time of harvest. Thus, virtually all of the Chls extracted after the $^{18}O_2$-labeling period were formed during the incubation in the controlled atmosphere. After the overnight greening period with $^{18}O_2$, the cultures visually appeared to contain somewhat less than half as much Chl as fully greened cultures. Control experiments in which the O_2 concentration of the solution was monitored with an O_2 electrode indicated that atmospheric O_2 was effectively removed from the reaction vessel by the flushing protocol and that the vessel was gas-tight when sealed. Furthermore, DCMU was added to the culture to inhibit photosynthetic O_2 evolution which would dilute the $^{18}O_2$ in the controlled atmosphere with photosynthetically-derived O_2. Together, these factors maintained the system in an essentially $^{16}O_2$-free state during the greening period.

Chl Purification. Reverse-phase HPLC was used to separate the pigments extracted from *Chlorella* cultures greened in the $^{18}O_2$-enriched atmosphere. A typical elution

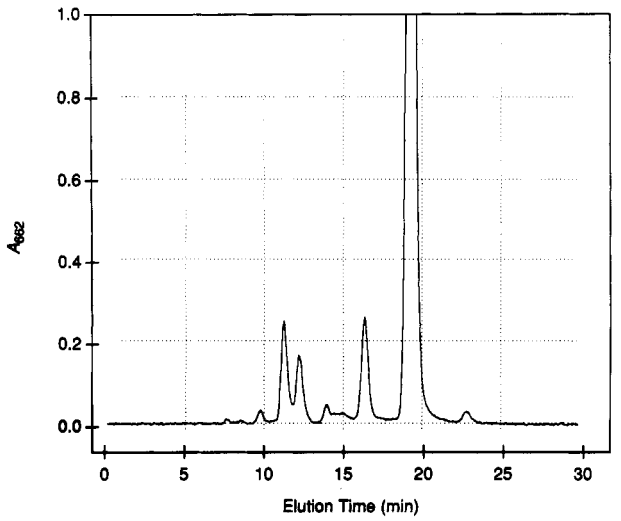

FIGURE 2: Reverse-phase HPLC elution profile of Chls extracted from *Chlorella* cells that were greened in an $^{18}O_2$-enriched atmosphere. Chl *b* and Chl *a* eluted at 11.2 and 19.3 min, respectively. Smaller peaks include the Chl *a* C-10 epimer and Chls bearing incompletely hydrogenated isoprene moieties, as discussed in the text.

profile is shown in Figure 2. The peaks were designated by comparison to published profiles (Shioi et al., 1983) and by measuring their absorption spectra with a flow-through diode array detector. Chls *b* and *a* eluted at 11.2 and 19.3 min, respectively. The Chl *a*:Chl *b* ratio was approximately 10. Because the greening process was not completed during the labeling period, significant quantities of Chl precursors were present. The expected Chl *a* precursors having incompletely hydrogenated isoprene moieties; i.e., the geranylgeranyl, dihydrogeranylgeranyl, and tetrahydrogeranylgeranyl esters of Chlide *a*, eluted at 12.4, 14.1, and 16.6 min, respectively. An analogous series of small peaks containing Chl *b*-like species was usually observed preceding the Chl *b* peak (Shioi & Sasa, 1983). Because Chl *b* and geranylgeranyl-Chlide *a* were not fully resolved, the trailing edge of the Chl *b* peak was discarded. Also apparent in the elution profile is the small peak attributed to the C-10 epimer of Chl *a*, which eluted at approximately 23 min.

Spectrophotometric Measurements. The absorption spectra of HPLC-purified Chl *a* and Chl *b* were recorded in methanol. Spectral maxima and minima (data not shown) were at the previously reported positions in this solvent (Mackinney, 1941). In an attempt to detect possible contamination of the Chl *b* sample by 10-hydroxy-Chl *a* or other Chl *a* allomers, its absorption spectrum was analyzed by interactive computer-aided Bessel deconvolution. No bands other than those attributable to Chl *b* were detected (data not shown).

Mass Spectroscopy. High-resolution mass spectra were obtained from the Chls extracted from *Chlorella* cells that were greened in the $^{18}O_2$-enriched atmosphere. The m/z values and relative peak intensities are shown in Table I. Because of the possibility of allomer formation (Schaber et al., 1984) and exchange of the Chl *b* formyl oxygen with the solvent during sample preparation, especially during procedures that would be required to remove the Mg atom and phytyl group, the mass spectra of the HPLC-purified Chls were obtained directly, without prior derivatization. This method introduces analytical complications due to the significant contributions of the two heavy isotopes of Mg and the ^{13}C of the phytyl group to the natural abundance mass spectra. Analysis of the Chl mass spectra is described in detail below.

Analysis of the Internal Standard Mass Signals. NPG, Na^+-$H(OCH(CH_3)CH_2)_nOH$, was used as the internal

Table I: Mass Spectral Data

	measured m/z (amu)	measured intensity (cps)	net relative intensity (% of sum)	natural abundance relative intensity (% of sum)
		Chl *a* Signals		
M	892.5347	8.58×10^5	6.79	41.81
M + 1	893.5374	1.21×10^6	9.74	31.66
M + 2	894.5425	3.83×10^6	31.45	17.87
M + 3	895.5470	3.36×10^6	27.59	6.74
M + 4	896.5487	1.94×10^6	15.81	1.55
M + 5	897.5507	8.50×10^5	6.72	0.37
M + 6	898.5530	2.69×10^5	1.90	
background		4.00×10^4		
		Chl *b* Signals		
M	906.5140	1.62×10^5	7.00	41.73
M + 1	907.5235	2.31×10^5	10.05	31.60
M + 2	908.5261	4.88×10^5	21.41	17.92
M + 3	909.5272	4.92×10^5	21.61	6.79
M + 4	910.5291	4.14×10^5	18.16	1.58
M + 5	911.5349	2.89×10^5	12.63	0.38
M + 6	912.5356	1.47×10^5	6.33	
M + 7	913.5464	6.75×10^4	2.81	
background		4.00×10^3		
		Standard Signals		
M	911.6264	3.72×10^5	60.58	60.03
M + 1	912.6289	1.88×10^5	30.26	31.26
M + 2	913.6323	5.97×10^4	9.16	8.71
background		4.00×10^3		

molecular weight standard in the mass spectroscopy. Some signals from the standard (where $n = 15$) overlap the (M + 5)–(M + 7) region of the Chl *b* mass spectrum (nominal masses 911–913). Fortunately, the masses of these standard peaks, at m/z values of 911.6264, 912.6289, and 913.6323, are sufficiently different from any signals that can be assigned to Chl *b* that they can easily be distinguished. These signals agree very closely with the m/z values for the major components of the standard signals, calculated from the atomic composition and natural isotopic abundances of the constituent atoms (Table II). The relative intensities of the signals also agree very closely with the calculated values for the standard signal cluster (Figure 3).

Relative Intensity Analysis of the Chl Mass Signals. Natural abundance mass spectra of Chl *a* and Chl *b* were calculated, on the basis of the atomic composition of the Chls and the natural abundances of their constituent atoms. The natural abundance of ^{13}C was adjusted from the nominal value of 1.1080% to 1.0806%, to take into account the average biological isotopic enrichment of 25‰ for ^{12}C that has been determined for fresh water chlorophyte algae (Galimov, 1985). The calculated natural abundance relative peak intensities for the Chl *a* and Chl *b* signal clusters are shown in Table I.

Because the mass spectra were expected to contain signals from both $M^{\bullet +}$ and $(M + H)^+$ Chl ions, the next step was to consider that Chl $(M + H)^+$ ions will have signal clusters similar to those of the $M^{\bullet +}$ ions, but with all peaks shifted upward by one mass unit. Chl ions derived from molecules that were labeled with one ^{18}O atom will have signal clusters similar to those of unlabeled Chl $M^{\bullet +}$ and $(M + H)^+$ ions, but with all masses shifted upward by two mass units. This analysis can be extended to Chl molecules labeled with two ^{18}O atoms. Calculated mass spectral signal clusters can be generated on the basis of arbitrary proportions of $M^{\bullet +}$ and $(M + H)^+$ ions and arbitrary degrees of labeling by one ^{18}O atom (for Chl *a*) or two ^{18}O atoms (for Chl *b*).

For Chl *a*, the experimentally determined spectrum was compared with a calculated spectrum that was generated on the basis of the above considerations. The composition of the

Table II: Relative Contributions, Masses, and Mass Differences of Major Components of the Signals from the Internal Standard

	measured m/z (amu)	component	ion	relative contribution (% of signal)	calculated m/z (amu)	absolute m/z difference (mamu)
M	911.6264	NPG	$M^{\bullet +}$	100.00	911.6283	1.9
M + 1	912.6289	^{13}C-NPG	$M^{\bullet +}$	96.82	912.6317	2.8
M + 2	913.6323	$^{13}C_2$-NPG	$M^{\bullet +}$	85.68	913.6350	2.7

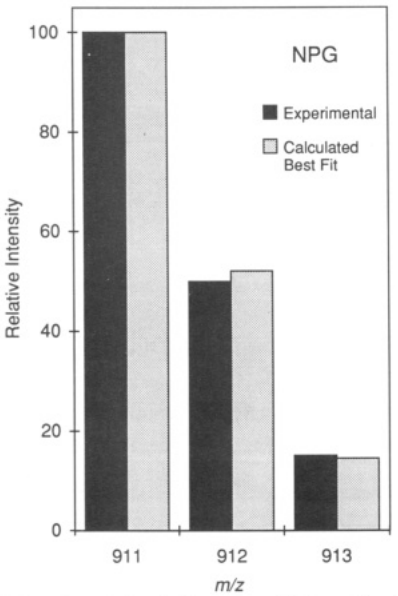

FIGURE 3: Experimental relative signal intensities in the mass spectrum of NPG used as an internal standard and the best-fit calculated spectrum.

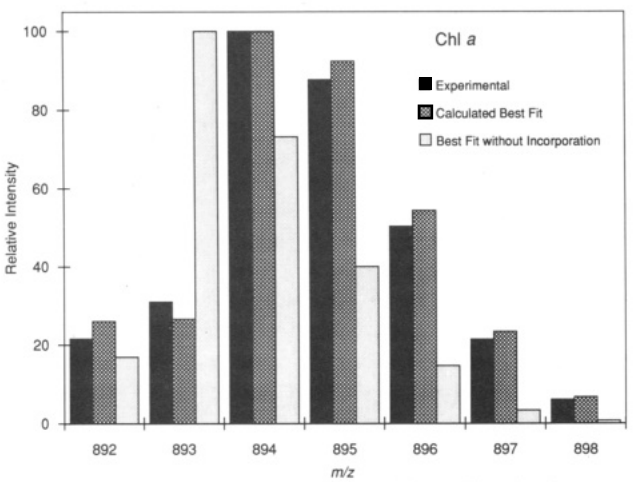

FIGURE 4: Experimental relative signal intensities in the mass spectrum of Chl *a*, the best-fit calculated spectrum, and the best fit obtained without ^{18}O incorporation allowed.

calculated spectrum was adjusted until a best fit to the experimental spectrum was obtained. The criterion for the best fit (figure of merit) was minimization of the sum of squares of the percent differences between the relative intensities of the experimental and calculated peaks for the M through M + 6 signals (nominal masses 892–898). The best fit (lowest figure of merit) was obtained with the calculated spectrum for Chl *a* that was 76.27% labeled with one ^{18}O atom (above natural abundance) and had 79.30% $M^{\bullet +}$ ions with the remainder $(M + H)^+$ ions. The figure of merit for this comparison was 6.81%.[2] In contrast, the best fit that was obtained when the calculated spectrum was constrained to have no ^{18}O labeling (above natural abundance) has a figure of merit of 1167.19%.[2] In Figure 4, the experimental data for Chl *a* are compared with the best-fit spectrum and the best fit possible without ^{18}O incorporation.

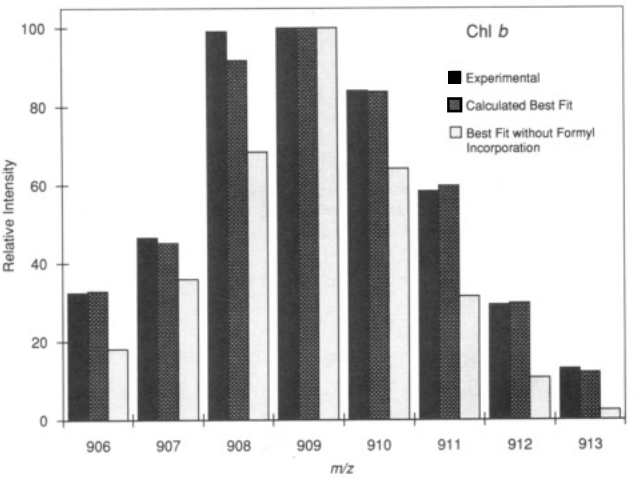

FIGURE 5: Experimental relative signal intensities in the mass spectrum of Chl *b*, the best-fit calculated spectrum, and the best fit obtained with incorporation of only 1 ^{18}O atom allowed.

For Chl *b*, the analysis was similar to that for Chl *a* except that the calculated spectra were allowed to contain arbitrary enrichments of two ^{18}O atoms. The calculations included the M through M + 7 signals (nominal masses 906–913). The best fit was obtained with the calculated spectrum for Chl *b* that was 58.21% labeled with one ^{18}O atom and 33.68% labeled with a second ^{18}O atom, and had 61.67% $M^{\bullet +}$ ions with the remainder $(M + H)^+$ ions. The figure of merit for this comparison was 1.12%.[2] In contrast, the best fit that was obtained when the calculated spectrum was constrained to have enrichment of only one ^{18}O atom has a figure of merit of 106.23%.[2] In Figure 5, the experimental data for Chl *b* are compared with the best-fit spectrum and the best fit possible with incorporation of only one ^{18}O atom.

The ratios of $M^{\bullet +}$ to $(M + H)^+$ ions in the calculated best-fit mass spectra are comparable to those previously reported for positive-ion FAB mass spectra of Chls (Brereton et al., 1983). The high proportion of molecular ions reflects the relative ease of radical cation formation for the Chls, expecially Chl *a*.

Molecular Mass Analysis of the Mass Signals. The high-resolution peak positions (m/z values) cannot be used directly to determine the compositions of Chl *a* and Chl *b* containing mixtures of labeled and unlabeled molecules because these mixtures produce spectra in which several components, with closely similar masses, contribute to each peak. However, after the percent of $M^{\bullet +}$ ions and percent of ^{18}O labeling were determined for the best fit calculated Chl *a* and Chl *b* spectra as described above, it was possible to calculate the relative contributions of the major components that contribute to each peak in the spectra, and then to compare the calculated masses of these components with the experimentally measured m/z values. Tables III and IV list all components that were calculated to contribute 10% or more to the total intensity of each peak in the high-resolution spectra of Chl *a* and Chl *b*, respectively, and the differences between the experimental and calculated m/z values. At the resolution to which the

Table III: Relative Contributions, Masses, and Mass Differences of All Components Calculated To Contribute 10% or More to the Chl *a* Signals

	measured *m/z* (amu)	component	ion	relative contribution (% of signal)	calculated *m/z* (amu)	absolute *m/z* difference (mamu)
M	892.5347	Chl *a*	$M^{\bullet+}$	100.00	892.5353	0.6
M + 1	893.5374	^{13}C-Chl *a*	$M^{\bullet+}$	59.00	893.5387	1.3
		Chl *a*	$(M + H)^+$	25.63	893.5431	5.7
		^{25}Mg-Chl *a*	$M^{\bullet+}$	12.64	893.5361	1.3
M + 2	894.5425	^{18}O-Chl *a*	$M^{\bullet+}$	83.72	894.5396	2.9
M + 3	895.5470	^{18}O-^{13}C-Chl *a*	$M^{\bullet+}$	54.46	895.5429	4.1
		^{18}O-Chl *a*	$(M + H)^+$	23.66	895.5474	0.4
		^{18}O-^{25}Mg-Chl *a*	$M^{\bullet+}$	11.67	895.5404	6.6
M + 4	896.5487	^{18}O-$^{13}C_2$-Chl *a*	$M^{\bullet+}$	27.28	896.5463	2.4
		^{18}O-^{13}C-Chl *a*	$(M + H)^+$	24.14	896.5507	2.0
		^{18}O-^{13}C-^{25}Mg-Chl *a*	$M^{\bullet+}$	21.85	896.5437	5.0
		^{18}O-^{26}Mg-Chl *a*	$M^{\bullet+}$	11.91	896.5371	11.6
M + 5	897.5507	^{18}O-^{13}C-^{26}Mg-Chl *a*	$M^{\bullet+}$	30.61	897.5405	10.2
		^{18}O-$^{13}C_2$-Chl *a*	$(M + H)^+$	16.61	897.5541	3.4
		^{18}O-^{26}Mg-Chl *a*	$(M + H)^+$	13.30	897.5449	5.8
		^{18}O-$^{13}C_3$-Chl *a*	$M^{\bullet+}$	12.28	897.5496	1.1
M + 6	898.5530	^{18}O-$^{13}C_2$-^{26}Mg-Chl *a*	$M^{\bullet+}$	31.50	898.5438	9.2
		^{18}O-^{13}C-^{26}Mg-Chl *a*	$(M + H)^+$	27.87	898.5483	4.7
		^{18}O-$^{13}C_3$-Chl *a*	$(M + H)^+$	11.18	898.5574	4.4

Table IV: Relative Contributions, Masses, and Mass Differences of All Components Calculated To Contribute 10% or More to the Chl *b* Signals[a]

	measured *m/z* (amu)	component	ion	relative contribution (% of signal)	calculated *m/z* (amu)	absolute *m/z* difference (mamu)
M	906.5140	Chl *b*	$M^{\bullet+}$	100.00	906.5146	0.6
M + 1	907.5235	Chl *b*	$(M + H)^+$	45.08	907.5224	1.1
		^{13}C-Chl *b*	$M^{\bullet+}$	43.58	907.5179	5.6
M + 2	908.5261	^{18}O-Chl *b*	$M^{\bullet+}$	67.92	908.5188	7.3
		^{13}C-Chl *b*	$(M + H)^+$	13.34	908.5258	0.3
		(10-OH-Chl *a*)	$M^{\bullet+}$		(908.5302)	(4.1)
M + 3	909.5272	^{18}O-Chl *b*	$(M + H)^+$	38.76	909.5266	0.6
		^{18}O-^{13}C-Chl *b*	$M^{\bullet+}$	37.47	909.5222	5.0
		(10-OH-Chl *a*)	$(M + H)^+$		(909.5381)	(10.9)
M + 4	910.5291	^{18}O-^{13}C-Chl *b*	$(M + H)^+$	27.82	910.5300	0.9
		$^{18}O_2$-Chl *b*	$M^{\bullet+}$	27.73	910.5231	6.0
		^{18}O-$^{13}C_2$-Chl *b*	$M^{\bullet+}$	13.20	910.5255	3.6
		^{18}O-^{13}C-^{25}Mg-Chl *b*	$M^{\bullet+}$	10.57	910.5230	6.1
		(10-OH-^{18}O-Chl *a*)]	$M^{\bullet+}$		(910.5345)	(5.4)
M + 5	911.5349	$^{18}O_2$-Chl *b*	$(M + H)^+$	24.18	911.5309	4.0
		$^{18}O_2$-^{13}C-Chl *b*	$M^{\bullet+}$	23.37	911.5264	8.5
		^{18}O-$^{13}C_2$-Chl *b*	$(M + H)^+$	11.51	911.5334	1.5
		(10-OH-^{18}O-Chl *a*)	$(M + H)^+$		(911.5423)	(7.4)
M + 6	912.5356	$^{18}O_2$-^{13}C-Chl *b*	$(M + H)^+$	29.30	912.5342	1.4
		$^{18}O_2$-$^{13}C_2$-Chl *b*	$M^{\bullet+}$	13.90	912.5298	5.8
		^{18}O-^{13}C-^{26}Mg-Chl *b*	$(M + H)^+$	11.17	912.5276	8.0
M + 7	913.5464	$^{18}O_2$-$^{13}C_2$-Chl *b*	$(M + H)^+$	21.50	913.5376	8.8
		$^{18}O_2$-^{26}Mg-Chl *b*	$(M + H)^+$	17.22	913.5284	18.0
		$^{18}O_2$-^{13}C-^{26}Mg-Chl *b*	$M^{\bullet+}$	16.65	913.5240	22.4

[a] Calculated values for 10-hydroxy–Chl *a* are shown in parentheses.

instrument was set (1 part in 10 000), the molecular weight discrimination was equal to 9 mamu in the Chl mass range. In almost all cases, the calculated major components contributing to the peaks have *m/z* values that are within the experimental resolution limits. Exceptions occur at some higher order peaks which contain many contributing components. Thus, although the high-resolution *m/z* values alone cannot be used to define the isotopic composition of the Chls, the experimental results are consistent with the ^{18}O-labeling values for Chl *a* and Chl *b* that were calculated from the peak intensity ratios.

The foregoing high-resolution mass spectroscopic results are consistent with high levels of incorporation of one ^{18}O into both Chl *a* and Chl *b* and a significant level of incorporation of a second ^{18}O into Chl *b*. It can be calculated that the incorporated ^{18}O must be derived directly from the $^{18}O_2$, rather than indirectly from $H_2{}^{18}O$ that was formed from the $^{18}O_2$ by cellular respiration during the incubation period. A total of 0.0089 mole atom of ^{18}O was present in the 100 mL of $^{18}O_2$ that was used to enrich the atmosphere. A total of 18.15 mole atoms of O was present in the 330 mL of aqueous medium in which the cells were suspended during the incubation. The atmospheric ^{18}O would be diluted over 2000-fold, which is beyond the limit of detection, if it had exchanged with H_2O in the medium. Therefore, the high levels of ^{18}O in Chl *a* and Chl *b* must have been achieved by direct incorporation from $^{18}O_2$.

DISCUSSION

The mass spectra clearly indicate that Chls formed by *Chlorella* cells in an $^{18}O_2$-enriched atmosphere contain ^{18}O that is derived from atmospheric $^{18}O_2$. Quantitative analysis of the mass spectra indicates that most Chl *a* molecules contain 1 mole atom of ^{18}O and that a significant fraction of the Chl *b* molecules contain 2 mole atoms of ^{18}O. The incorporation of ^{18}O into both Chl *a* and Chl *b* is consistent with a previous

report which showed that the isocyclic ring keto oxygen of the Chl precursor, Pchlide, is derived from O_2 in etiolated cucumber cotyledons (Walker et al., 1989). Furthermore, the incorporation of a second mole atom of ^{18}O into Chl *b* indicates that the formyl oxygen of Chl *b* is also derived from O_2.

For the above conclusion regarding the origin of the formyl oxygen of Chl *b* to be valid, it was important to ensure that the Chl *b* sample used for mass spectral analysis was free of 10-hydroxy-Chl *a*. This Chl *a* derivative (Figure 1) has a composition of $C_{55}H_{72}N_4O_6Mg$ and a calculated mass of 908.5302, which differs from that of singly-^{18}O-labeled Chl *b* ($C_{55}H_{70}N_4O_6Mg$) by only 11.4 mamu; the mass of singly-^{18}O-labeled 10-hydroxy-Chl *a* differs from that of doubly-^{18}O-labeled Chl *b* by the same amount. These m/z values cannot be reliably distinguished because the mass difference is near the resolution limit of the mass spectra. 10-Hydroxy-Chl *a* can be formed in the presence of methanol under mild conditions (Holt, 1958; Schaber et al., 1984). However, the HPLC system that was used has been demonstrated to effectively separate 10-hydroxy-Chl *a* from Chl *b* (Shioi et al., 1983; Schaber et al., 1984). The absorption spectrum of 10-hydroxy-Chl *a* is similar to that of Chl *a* and readily distinguished from that of Chl *b*. No Chl *a*-like absorption bands were detected in the absorption spectrum of HPLC-purified ^{18}O-labeled Chl *b*. Therefore, significant contamination of the Chl *b* sample with Chl *a* or its 10-hydroxy derivative is excluded. Any hydroxylation of Chl *b* that might have occurred after the HPLC purification step would yield a product with a mass 16 amu higher than that of Chl *b*, and its presence would not interfere with the mass spectral analysis. Other known Chl derivatives or precursors, such as those containing partially hydrogenated side chains or two vinyl groups, would have been separated from Chl *a* and Chl *b* by HPLC. Moreover, these compounds would be at least 2 amu lighter than the mature underivatized Chls, and their presence would not interfere with the mass spectral analysis. Therefore, it appears that the Chl *b* produced by *Chlorella* in an $^{18}O_2$-enriched atmosphere had a significant degree of incorporation of 2 mole atoms of ^{18}O.

It is very improbable that any of the oxygen atoms in the carboxymethyl and carboxyphytyl moieties of Chl *b* were labeled by $^{18}O_2$ in these experiments. First, it is known that ester bond bridge oxygens of these moieties are derived from the tetrapyrrole, rather than the esterifying alcohols (Emery & Akhtar, 1987). The carboxyl groups of tetrapyrroles in plants and algae arise from the γ-carboxyl group of glutamate (Beale & Weinstein, 1990), the oxygen of which ultimately derived from water via acetyl-coenzyme A. Second, a corresponding incorporation of a second ^{18}O atom was not detected in Chl *a*, even though Chl *a* and Chl *b* are structurally identical at these positions. With the Chl *b* keto oxygen ^{18}O-labeled as predicted, the only oxygen unaccounted for in Chl *b* is that of the formyl group. Therefore, it appears that the second ^{18}O atom in Chl *b* was incorporated into the formyl group.

Over 76% of the Chl *a* formed by *Chlorella* in the $^{18}O_2$-enriched atmosphere was labeled with 1 mole atom of ^{18}O. This incorporation is lower than the 97–98% labeling that would be expected from the isotopic purity of the $^{18}O_2$ introduced into the incubation chamber. Incomplete labeling could result from residual $^{16}O_2$ in the reaction vessel and cells, slow leakage of atmospheric $^{16}O_2$ into the vessel during the incubation period, and/or dilution of the $^{18}O_2$ in the vessel by low levels of photosynthetic $^{16}O_2$ produced by the cells, which might not have been completely inhibited throughout the incubation period by the administered concentration of DCMU. The incorporation of ^{18}O into the isocyclic ring keto oxygen of Chl *b* was 58%, which is somewhat less than for Chl *a*. The difference can be explained by the fact that, as has been observed in other rapidly greening, dark-grown cells (Anderson & Boardman, 1964), Chl *b* begins to accumulate later than Chl *a* after transfer of dark-grown *Chlorella* cells to the light (M. A. Schneegurt and S. I. Beale, unpublished results). Dilution of the $^{18}O_2$ by leakage of atmospheric $^{16}O_2$ into the chamber and/or by photosynthetically-produced $^{16}O_2$ would be cumulative and would therefore have a greater effect on lowering the incorporation of ^{18}O into Chl *b* relative to the effect on Chl *a*.

The apparent incorporation of ^{18}O into the formyl oxygen of Chl *b* is 34%, which is less than the incorporation into the keto oxygen of either Chl *a* or Chl *b* and much less than would be expected from the $^{18}O_2$ enrichment in the controlled atmosphere. It must be stressed that the Chl *b* formyl group is expected to undergo reversible hydration in aqueous solvents, which would cause exchange of the formyl oxygen with that of H_2O. For a given Chl *b* molecule, each round of hydration and dehydration of the formyl group has a 50% probability of exchanging the formyl oxygen for that of H_2O. Although the experimental strategy of minimizing exposure of the Chls to acids and aqueous solvents was designed to minimize the loss of label by solvent exchange, some loss of the formyl label was unavoidable. Because the total number of mole atoms of ^{18}O in the gas phase of the sealed incubation apparatus was less than 0.05% of the number of mole atoms of ^{16}O in the aqueous phase, incorporation into Chl *b* via conversion to H_2O would have diluted the ^{18}O to undetectable levels of enrichment. Therefore, the measured enrichment of ^{18}O that remained in the Chl *b* formyl oxygen after purification could have arisen only by direct biosynthetic incorporation of $^{18}O_2$, and the actual level of incorporation before loss by solvent exchange was probably much greater than 34%. The results thus indicate that the Chl *b* formyl oxygen is derived from O_2.

Formally, the Chl *b* mass spectrum can also be interpreted to indicate the opposite relative ^{18}O incorporation levels, i.e., 34% incorporation into the keto group and 58% incorporation into the formyl group. However, this interpretation is inconsistent with the high ^{18}O incorporation into the Chl *a* keto group and the predicted exchangeability of the Chl *b* formyl oxygen. In any case, the results would still indicate that the Chl *b* formyl oxygen atom is derived from O_2.

In conclusion, the results indicate that the conversion of the methyl group to a formyl group during Chl *b* biosynthesis is an oxygenation reaction. The determination that O_2 is the source of the Chl *b* formyl oxygen will provide a useful guide for future experiments on the mechanism of Chl *b* formation and the enzymes that catalyze this biosynthetic reaction.

ACKNOWLEDGMENT

We are greatly indebted to M. Collins and J. Occolowitz for obtaining the mass spectra and to J. E. Hunt for providing a preprint of the mass spectroscopy procedure and early guidance. We thank M. J. Coghlan, S. Rieble, H. Scheer, K. M. Smith, C. Waldron, and J. P. Wright for help and suggestions and D. L. Cullen for performing preliminary experiments.

REFERENCES

Akoyunoglou, G., Argyroundi-Akoyunoglou, J. H., Michel-Wolwertz, M. R., & Sironval, C. (1967) *Chim. Chron. 32*, 5–8.

Anderson, J. M., & Boardman, N. K. (1964) *Aust. J. Biol. Sci. 17*, 93–101.
Aronoff, S., & Kwok, E. (1977) *Can. J. Biochem. 55*, 1091–1095.
Beale, S. I., & Weinstein, J. D. (1990) in *Biosynthesis of Heme and Chlorophylls* (Dailey, H. A., Ed.) pp 287–391, McGraw-Hill, New York.
Bednarik, D. P., & Hoober, J. K. (1985) *Science 230*, 450–453.
Bednarik, D. P., & Hoober, J. K. (1986) in *Regulation of Chloroplast Differentiation* (Akoyunoglou, G., & Senger, H., Eds.) pp 105–114, Alan R. Liss, New York.
Benz, J., Lempert, U., & Rüdiger, W. (1984) *Planta 162*, 215–219.
Brereton, R. G., Bazzaz, M. B., Santikarn, S., & Williams, D. H. (1983) *Tetrahedron Lett. 24*, 5775–5778.
Bryan, G. W., & Bogorad, L. (1963) *Plant Cell Physiol. 4* (*Suppl.*), 399–405.
Castelfranco, P. A., & Beale, S. I. (1983) *Annu. Rev. Plant Physiol. 34*, 241–278.
Duggan, J. X., & Rebeiz, C. A. (1982) *Biochim. Biophys. Acta 714*, 248–260.
Emery, V. C., & Akhtar, M. (1987) *Biochemistry 26*, 1200–1208.
Galimov, E. M. (1985) *The Biological Fractionation of Isotopes*, Academic Press, New York.
Godnev, T. N., Ratfarb, R. M., & Shlyk, A. A. (1960) *Dokl. Akad. Nauk. SSSR 130*, 663–666.
Holt, A. S. (1958) *Can. J. Biochem. Physiol. 36*, 439–456.
Hunt, J. E., & Michalski, T. J. (1990) in *Chlorophylls* (Scheer, H., Ed.) pp 835–853, CRC Press, Boca Raton, FL.
Mackinney, G. (1941) *J. Biol. Chem. 140*, 315–322.
Oelze-Karow, H., Kasemir, H., & Mohr, H. (1978) in *Chloroplast Development* (Akoyunoglou, G., & Argyroundi-Akoyunoglou, J. H., Eds.) pp 787–792, Elsevier, Amsterdam.
Oelze-Karow, H., & Mohr, H. (1978) *Photochem. Photobiol. 27*, 189–193.
Schaber, P. M., Hunt, J. E., Fries, R., & Katz, J. J. (1984) *J. Chromatogr. 316*, 25–41.
Shioi, Y., & Sasa, T. (1983) *Biochim. Biophys. Acta 756*, 127–131.
Shioi, Y., Fukae, R., & Sasa, T. (1983) *Biochim. Biophys. Acta 722*, 72–79.
Shlyk, A. A. (1971) *Annu. Rev. Plant Physiol. 22*, 169–184.
Shlyk, A. A., Vlasenok, L. I., Akhramovich, N. I., Vrubel, S. V., & Akulovich, E. M. (1975) *Dokl. Akad. Nauk. SSSR 221*, 1234–1236.
Walker, C. J., Mansfield, K. E., Smith, K. M., & Castelfranco, P. A. (1989) *Biochem. J. 257*, 599–602.
Weinstein, J. D., & Beale, S. I. (1985) *Arch. Biochem. Biophys. 237*, 454–464.

Registry No. Chl *b*, 519-62-0; Chl *a*, 479-61-8; O_2, 7782-44-7.